3D Digital Filtering of Volumetric Images

Dimitar G. Valchev

Abstract – **This paper shows three different kinds of three-dimensional (3D) digital filters for processing of volumetric images. Ideal impulse responses are given for a separable, a non-separable and a semi-separable 3D filter.**

Keywords – **Digital filters, Digital image processing.**

I. INTRODUCTION

Volumetric images are characteristic to many applications in computer tomography and magnetic resonance imaging, as well as in subsurface sensing and imaging of various hidden spaces. These volumetric images are represented as three-dimensional (3D) arrays of voxel values. They give realistic representations of solid shapes as true 3D images, not just two-dimensional (2D) projections onto a planar display consisting of pixels. Being essentially 3D signals, volumetric images are subject to 3D signal processing [1]. The various filtering techniques from one-dimensional (1D) and 2D digital signal processing (DSP) [2, 3] may easily be extended to three dimensions. Filters used in 3D volumetric digital image processing share many common properties with their 1D counterparts and hence the various design approaches for 3D filters can be closely related to 1D and 2D algorithms.

On the other hand, there are some differences from the 1D and 2D cases, due to the additional dimensionality in 3D digital filtering. 3D filters are characterized by more degrees of freedom that can be used to achieve design optimality. Also, the available mathematical tools are more restrictive which further complicates the design process. Since 3D polynomials can not be factorized, the designer must consider the implementation aspect, especially separability. Again, due to the increased dimensionality and hence number of degrees of freedom, the separable filter can be fully separable in the three dimensions, or semi-separable – non-separable in two dimensions but separable in the third one.

The rest of the paper is organized as follows. Section II gives the basics of 3D digital filtering. Section III presents different kinds of separability in 3D digital filters. Section IV concludes the paper pointing at further research aspects in 3D digital filtering.

II. BASICS OF 3D DIGITAL FILTERING

Common to all 3D digital filtering techniques is the frequency response of an ideal lowpass 3D filter. Starting with it, various techniques known from 1D DSP [4] can be applied. Then, based on the derived impulse response, various highpass, bandpass and bandstop filters can be designed. The impulse responses of the 3D filters as well as the volumetric images are defined on generally rectangular sampling grids. The sampling grids can also be non-rectangular [2, 3] depending on optimality considerations. This paper considers rectangular sampling grids.

A. Ideal Lowpass Filter

The starting point for designing a digital filter is the ideal lowpass filter spectral characteristic from which different highpass, bandpass and bandstop filter configurations can be derived. Similarly to the digital filters in 2D signal and image processing [2, 3], the 3D volumetric image filters can also be separable with rectangular support and non-separable. In addition, the 3D filters can be also semi-separable with cylindrical support.

B. Three kinds of pass bands in 3D filters

The performance difference among a separable, a semi-separable and a non-separable filter can be perceived through the spectral characteristics along different directions in 3D space. On the one hand, the separable filter is simply designed; its impulse response is equal to the product of the marginal impulse responses along the three spatial axes which determines independent spectral characteristics along the three axes. Its passband is rectangular which means that this kind of filter would pass higher frequencies along the diagonal directions of the rectangle, compared to the frequencies along each frequency axis.

On the other hand, the non-separable filter offers spectral characteristics along the different directions which are no longer independent. In particular, the non-separable filter with spherical passband offers equal spectral characteristics along any direction in 3D space. This may be very important especially in computed tomography and magnetic resonance imaging where the data details are equally important in all directions.

Between the performance of the separable and the non-separable 3D FIR filter is the semi-separable filter with cylindrical support. It has non-independent spectral characteristics in one plane and independent ones in the direction perpendicular to that plane. This can play role in subsurface imaging where a 3D image is constructed from many 2D image slices where the slicing can be performed at a much lower rate compared to the 2D sampling rate for the images within each slice.

The 3D sampling grid and the three kinds of support regions are depicted in Fig. 1.

Dimitar G. Valchev is with the Department of Radioengineering, Technical University of Varna, Varna 9010, Bulgaria, E-mail: D.Valchev@tu-varna.bg

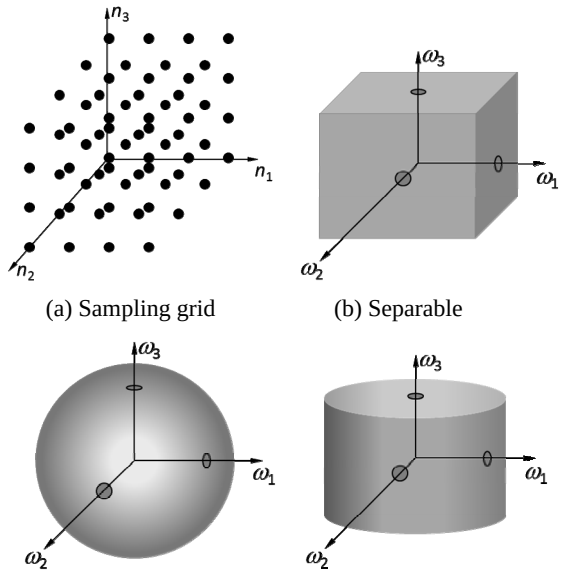

(a) Sampling grid (b) Separable

(c) Non-separable (d) Semi-separable

Fig. 1. 3D sampling grid and support regions for separable, non-separable and semi-separable ideal 3D lowpass filters

III. THREE KINDS OF SEPARABILITY IN 3D FILTERS

The rectangular passband defines a fully separable 3D filter. The impulse response of such a filter is given by [1]

$$h_r(n_1,n_2,n_3)=\frac{\sin\omega_{c_1}n_1}{\pi n_1}\frac{\sin\omega_{c_2}n_2}{\pi n_2}\frac{\sin\omega_{c_3}n_3}{\pi n_3} \tag{1}$$

for $-\infty < n_1, n_2, n_3 < \infty$, where ω_{c_1}, ω_{c_2} and ω_{c_3} are the cut-off spatial frequencies along the corresponding three frequency axes ω_1, ω_2 and ω_3 shown in Fig. 1 (a). For $\omega_{c_1}=\omega_{c_2}=\omega_{c_3}=\omega_c$, the filter's passband turns into cubic.

The spherical passband defines a non-separable 3D filter. The impulse response of such a filter is given by [1]

$$h_s(n_1,n_2,n_3)=\frac{\omega_c j_1\left(\omega_c\sqrt{n_1^2+n_2^2+n_3^2}\right)}{4\pi\left(n_1^2+n_2^2+n_3^2\right)} \tag{2}$$

where ω_c is the cut-off spatial frequency which is the same along the three frequency axes ω_1, ω_2 and ω_3 shown in Fig. 1 (b), and $j_1(x)$ is the first-order spherical Bessel function of the first kind, also equal to $\sin(x)/x^2 - \cos(x)/x$ [5].

The cylindrical passband defines a semi-separable 3D filter. The impulse response of such a filter is given by (details in the Appendix)

$$h_c=\frac{\omega_{c_1}\sin\omega_{c_3}n_3}{2\pi^2 n_3\sqrt{n_1^2+n_2^2}}J_1\left(\omega_{c_1}\sqrt{n_1^2+n_2^2}\right) \tag{3}$$

where ω_{c_1} and ω_{c_3} are the cut-off spatial frequencies along the corresponding three frequency axes ω_1, ω_2 and ω_3 shown in Fig. 1 (c). Here, without loss of generality it is assumed that the 3D fiter is non-separable in the n_1 and n_2 axes while separable in the n_3 axis. Any other orientation of the lowpass spatial spectral cylinder is also possible for a 3D filter characterized by a semi-separability in its arguments.

IV. CONCLUSION

This paper gives ideal impulse responses for three kinds of 3D digital filters for volumetric image processing: a separable, a non-separable and a semi-separable one. The separable filter is characterized by a rectangular passband, the non-separable filter is characterized by a spherical passband, and the semi-separable filter is characterized by a cylindrical passband. Such filters are applicable in various 3D subsurface sensing and imaging applications. Future work will focus on filter design approaches for volumetric digital image processing.

APPENDIX

This Appendix outlines the derivation of the impulse response of an ideal lowpass filter with a cylindrical passband. The frequency response of such a filter is given by

$$H_c(\omega_1,\omega_2,\omega_3)=\begin{cases}1, & \sqrt{\omega_1+\omega_2}\le\omega_{c_1},\ |\omega_3|\le\omega_{c_3},\\ 0, & \text{else},\end{cases} \tag{4}$$

in the frequency cube $[-\pi,+\pi]^3$. The ideal impulse response of the filter is derived by taking the inverse 3D Fourier transform of this function in the frequency domain [2]:

$$\begin{aligned}h_c&=\frac{1}{(2\pi)^3}\int_{-\pi}^{\pi}\iint_{\sqrt{\omega_1+\omega_2}\le\omega_{c_1}}1e^{j(\omega_1n_1+\omega_2n_2+\omega_3n_3)}d\omega_1d\omega_2d\omega_3\\&=\frac{1}{(2\pi)^3}\int_{-\pi}^{\pi}e^{j\omega_3n_3}d\omega_3\iint_{\sqrt{\omega_1+\omega_2}\le\omega_{c_1}}e^{j(\omega_1n_1+\omega_2n_2)}d\omega_1d\omega_2\end{aligned} \tag{5}$$

which reduces to [2, 5]

$$h_c=\frac{\omega_{c_1}}{2\pi\sqrt{n_1^2+n_2^2}}J_1\left(\omega_{c_1}\sqrt{n_1^2+n_2^2}\right)\frac{\sin\omega_{c_3}n_3}{\pi n_3}. \tag{6}$$

ACKNOWLEDGEMENT

This work is supported by the state budget of Technical University of Varna, research project # NP4/2011.

REFERENCES

[1] D. G. Valchev, "Volumetric image processing by 3D filters", *Internat. Sci. Conf. on Communications, Electromagnetics and Medical Applications CEMA'2010, Athens, Greece*, October 7–9, 2010, pp. 62–64.

[2] J. Woods, *Multidimensional signal, image and video processing and coding*, Elsevier Academic Press, 2006.

[3] D. Dudgeon, R. Mersereau, *Multidimensional digital signal processing*, Prentice Hall, 1990.

[4] J. Proakis, D. Manolakis, *Digital Signal Processing: Principles, Algorithms and Applications*, Prentice Hall, 2007.

[5] M. Abramowitz, I. Stegun, *Handbook of mathematical functions with formulas, graphs and mathematical tables*, Dover, 1972.